Article ID: 1006-8775(2012) 02-0162-10

MICROPHYSICAL CHARACTERISTICS OF THE RAINDROP SIZE DISTRIBUTION IN TYPHOON MORAKOT (2009)

CHEN Bao-jun (陈宝君), WANG Yuan (王　元), MING Jie (明　杰)

(Key Laboratory of Mesoscale Severe Weather/MOE, and School of Atmospheric Sciences, Nanjing University, Nanjing 210093 China)

Abstract: Microphysical characteristics of the raindrop size distribution (RSD) in Typhoon Morakot (2009) have been studied through the PARSIVEL disdrometer measurements at one site in Fujian province, China during the passage of the storm from 7 to 10 August 2009. The time evolution of the RSD reveals different segments of the storm. Significant difference was observed in the microphysical characteristics between the outer rainband and the eyewall; the eyewall precipitation had a broader size distribution (a smaller slope) than the outer rainband and eye region. The outer rainband and the eye region produced stratiform rains while the eyewall precipitation was convective or mixed stratiform-convective. The RSD was typically characterized by a single peak distribution and well represented by the gamma distribution. The relations between the shape (μ) and slope (Λ) of the gamma distribution and between the reflectivity (Z) and rainfall rate (R) have been investigated. Based on the N_W–D_m relationships, we suggest that the stratiform rain for the outer rainband and the eye region was formed by the melting of graupel or rimed ice particles, which likely originated from the eyewall clouds.

Key words: tropical cyclone; Morakot; raindrop size distribution; microphysics; PARSIVEL

CLC number: P444 **Document code:** A **doi:** 10.3969/j.issn.1006-8775.2012.02.006

1 INTRODUCTION

Heavy precipitation and strong winds associated with landfalling typhoons often cause tremendous loss of property and human lives. A typical example is Typhoon Morakot in August 2009, which brought record-breaking torrential rainfall over the island of Taiwan in 50 years[1] and claimed more than 600 lives with more than 200 people missing and an estimated $3.3 billion in damages[2]. Morakot also caused more than $1.3 billion property loss in mainland China. Given the huge impacts of Morakot, several studies have been conducted to investigate the factors that contributed to the heavy rainfall[1, 3], and explore the predictability and techniques that could improve the numerical weather prediction (NWP)[2, 4-6].

Information about the raindrop size distribution (RSD) is essential for understanding precipitation microphysics, estimating rainfall, and improving microphysics parameterizations in NWP models. Over the past several decades, numerous studies have documented the microphysical characteristics of the RSD for various rain types and climatic regimes using the observed disdrometer data[7-13]. Only a few studies focused on the RSD characteristics of tropical cyclones[14-15].

Herein we report the RSD characteristics of Typhoon Morakot based on disdrometer data at a 1-min time resolution observed in Fujian province, China, during the passage of the storm from 7 to 10 August 2009. The primary goals are to better understand the microphysics of the Morakot precipitation, and to investigate the difference between the RSD characteristics within typhoon systems.

2 DATA AND METHODOLOGY

2.1 *Instrumentation and data*

The RSD data analyzed in this study were collected with an OTT PARSIVEL disdrometer manufactured by the company OTT Messtechnik, Germany. Battaglia et al.[16] provided a detailed description of this instrument. Briefly, the instrument is a ground-based optical disdrometer that was

Received 2011-09-30; **Revised** 2012-02-15; **Accepted** 2012-04-15

Foundation item: National Natural Science Foundation of China (40730948, 40830958, 40921160382); National Grand Fundamental Research 973 Program of China (2009CB421502)

Biography: CHEN Bao-jun, Associate Professor, primarily undertaking research on cloud and precipitation physics.

Corresponding author: WANG Yuan, e-mail: yuanasm@nju.edu.cn

designed to count and measure simultaneously the fall speed and size of precipitation particles. The core element of the instrument is an optical sensor that produces a horizontal sheet of light (180-mm long, 30-mm wide, and 1-mm high). PARSIVEL can measure sizes up to about 26 mm and uses 32 size bins of different widths, ranging from 0.125 to 3 mm. The lowest two size bins are not used at all, because of their low signal-to-noise ratios. Exclusive of the first two bins, the range of particle sizes that can be measured spans from 0.3 to 26 mm in diameter. The smallest and largest detectable fall velocity is about 0.05 m s^{-1} and 21 m s^{-1}, respectively. The velocity is also subdivided into 32 bins with different widths, ranging from 0.1 to 3.2 m s^{-1}. PARSIVEL detects and identifies 8 different precipitation types as drizzle, mixed drizzle/rain, rain, mixed rain/snow, snow, snow grains, ice pellets and hail, according to the WMO, SYNOP, METAR and NWS weather codes. Yuter et al.[17] confirmed that PARSIVEL can be exploited as a present weather sensor because of its capability to distinguish rain, snow, and wet snow. In China, using the PARSIVEL disdrometer data, Niu et al.[12] analyzed the distributions of raindrop sizes and fall velocities for convective and stratiform rains in a semiarid plateau climate in Ningxia region, and Chen et al.[18] investigated microphysical characteristics of freezing rain during a freezing precipitation event on 27 January 2008 in Anhui province.

The particle diameter as measured by the PARSIVEL disdrometer is calculated from the maximum reduction of the voltage. A spheroid model is used to estimate the size of the particles as a function of voltage reduction. So, the particle sizes directly derived by the instrument, defined as the PARSIVEL size, are equivalent sphere diameter. However, the particle sizes frequently overestimate the large raindrop diameter[16, 19, 20]. To minimize the potential instrument error, the observed data herein are corrected following the method of Battaglia et al.[16]. In this scheme, particles below 1-mm equivalent sphere diameter D_{eq}^{PAR} are assumed to be spheres, where the superscript PAR stands for PARSIVEL. In the range from 1 to 5 mm, all raindrops are assumed to be horizontally oriented oblate spheroids with axial ratio a_r^{PAR} (defined as the ratio of height to width) linearly varying from 1 to 0.7, that is,

$$a_r^{\mathrm{PAR}} = 1.075 - 0.075 D_{\mathrm{eq}}^{\mathrm{PAR}}. \quad (1)$$

For particles with diameters above 5 mm, the axial ratio is kept constant at a value of 0.7.

The PARSIVEL disdrometer was installed on a mobile platform. The site of the measurement is located in Ningde, Fujian province, China, with latitude and longitude of 26.66°N and 119.55°E respectively. Continuous measurements were taken from 2100 Beijing Standard Time (BST) 6 August to 0746 BST 10 August, 2009. Figure 1 shows the best tracks of Typhoons Morakot and Goni from the Shanghai Typhoon Institute and the location of the observational site. The best track shows that Morakot was formed on 2 August, 2009. It reached its peak intensity, with winds of 150 km h^{-1} (a Category 2 hurricane), early on 7 August, and made landfall over Taiwan late on the same day. It stayed over Taiwan for about a day and then moved over the Taiwan Strait for about a day, subsequently making landfall over Xiapu, Fujian province, at 1620 BST 9 August. The typhoon weakened and dissipated on 11 August. During its passage over Fujian, Typhoon Morakot passed through the disdrometer site.

The disdrometer dataset used in this work consists of an about 47-h time series of 1-min drop size and fall speed distributions from 2025 BST 7 August to 0430 BST 10 August 2009. To minimize potential instrumental artifacts, raindrops in the lowest two size and velocity bins were discarded. Furthermore, the velocity-size relationship given by Gunn and Kinzer[21] that has been adjusted to local air density was used to identify potentially erroneous data using a 3σ criterion, that is, discarding the raindrops of any diameters with velocities 3 times the standard deviation of velocity calculated from every 10 consecutive samples at the corresponding diameters.

2.2 *Methodology*

Drop size distributions were fit with the well-known gamma function suggested by Ulbrich[22] as given by

$$N(D) = N_0 D^{\mu} \exp(-\Lambda D), \quad (2)$$

where D (mm) is the drop diameter, $N(D)$ (mm^{-1} m^{-3}) is the number of drops per unit volume per unit size interval, N_0 ($mm^{-1-\mu}$ m^{-3}) is the number concentration parameter, μ is the shape parameter, and Λ (mm^{-1}) is the slope parameter. The governing parameters in Eq. (2) were estimated from the second, fourth, and sixth moments of the observed distributions, respectively, using the truncated moment method described by Vivekanandan et al.[23]. Specifically, for the gamma model, the nth-order moment of the drop size distributions is expressed as

$$M_n = \int_{D_{\min}}^{D_{\max}} D^n N(D) dD = N_0 \frac{\Gamma(\mu + n + 1)}{\Lambda^{\mu+n+1}}. \quad (3)$$

The $N(D)$ (mm^{-1} m^{-3}) at a discrete instant of time has been calculated from the PARSIVEL disdrometer counts using the following equation,

$$N(D_i) = \sum_{j=1}^{32} \frac{n_{ij}}{A \cdot \Delta t \cdot V_j \cdot \Delta D_i}, \quad (4)$$

where n_{ij} is the number of drops reckoned in the size bin i and velocity bin j, A (m^2) and Δt (s) are the

sampling area and time, D_i (mm) is the drop diameter for the size bin i and ΔD_i is the corresponding diameter interval (mm), V_j (m s^{-1}) is the fall speed for the velocity bin j.

Given the RSD, the integral rainfall parameters of interest in this work can be computed, including the radar reflectivity factor Z (mm^6 m^{-3}) and rain rate R (mm h^{-1}) as given by

$$Z = \sum_{i=1}^{32} N(D_i) D_i^6 \Delta D_i , \quad (5)$$

$$R = \frac{6\pi}{10^4} \sum_{i=1}^{32} \sum_{j=1}^{32} V_j N(D_i) D_i^3 \Delta D_i . \quad (6)$$

Other two parameters of interest are the mass-weighted mean diameter D_m (mm) computed as the ratio of the 4th to 3rd moment of the size distribution:

$$D_m = \frac{M_4}{M_3}, \quad (7)$$

and the generalized intercept parameter N_w (mm^{-1} m^{-3}) defined by Bringi et al.[24]:

$$N_w = \frac{4^4}{\pi \rho_w} \left(\frac{10^3 W}{D_m^4} \right), \quad (8)$$

where ρ_w (1.0 g m^{-3}) represents the density of water and W (g m^{-3}) represents the liquid water content for the corresponding size distribution.

3 RAINDROP SIZE DISTRIBUTION

CHARACTERISTICS

Precipitation in tropical cyclones has both convective and stratiform components[25]. Figure 2 presents the N_w–D_m pairs based on all disdrometer data. Meanwhile, for clarity we also superimposed the Bringi et al.'s result of stratiform rain (shown as a solid straight line) and contours of rainfall rate. One can see that nearly 50% of N_w–D_m points fall in the stratiform rain area defined by Bringi et al.[24] with rain rate smaller than 3 mm h^{-1}. For constant rain rate, there was an inverse relationship between logarithmic N_w and D_m. Considering microphysical perspective in tropical cyclones, convective rains are generally produced by coalescence of drops, while stratiform rains are generated by melting of graupel and rimed ice particles or aggregates[25]. The variation in the N_w–D_m values, suggested by Bringi et al.[24], reflects the different microphysical formation mechanisms of stratiform rain, due to melting of large dry snowflakes (larger D_m and smaller N_w) versus melting of tiny graupel or smaller rimed ice particles (smaller D_m and larger N_w). From Figure 2, we can see that most N_w points were below D_m=1.5 mm and centered around 0.8 mm with the values of logarithmic N_w ~ 4. Thus, so large N_w and small D_m in the present work indicate that the stratiform precipitation was formed by the melting of tiny, compact graupel or rimed ice particles but not the melting of large, low-density snowflakes.

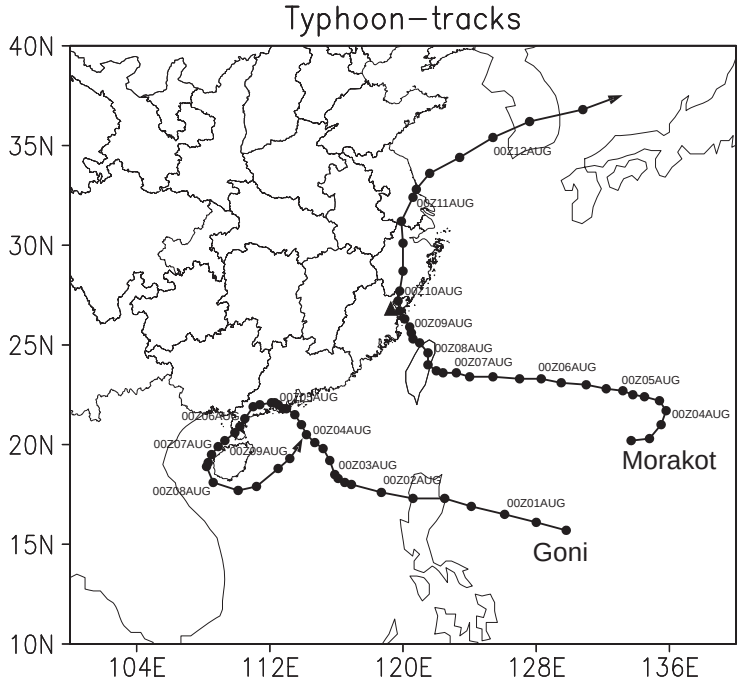

Figure 1. Observed best track of Typhoons Morakot and Goni are marked every 6 h. The location of the PARSIVEL disdrometer is indicated by the triangle.

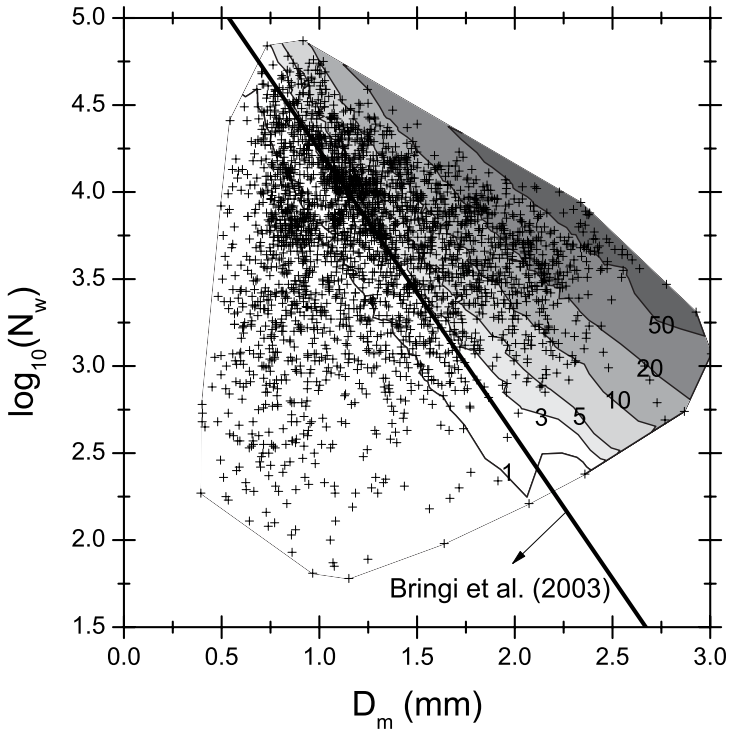

Figure 2. Scatterplot of the generalized number concentration N_w (mm^{-1} m^{-3}) versus the mass-weighted mean diameter Dm (mm) with contours of rainfall rate (mm h^{-1}). The solid straight line is the regression relation of Bringi et al. (2003) for stratiform rain.

To further investigate precipitation characteristics (convective vs. stratiform) from RSD during the passage of Morakot, for a given sample's D_m, the corresponding N_w was derived using the N_w–D_m regression relation of Bringi et al.[24] for stratiform rains. If the sample's N_w is smaller than that of Bring et al.[24], rainfall is identified as stratiform; otherwise, rainfall is convective. The results are shown in Figure 3. The total number concentration N_T, rain intensity R, liquid water content W, and radar reflectivity Z are also presented in the figure. The time series of these integral rainfall parameters revealed four distinct segments: the outer rainbands (072025–081035), eyewalls before landfall (081054–091619), eyes (091620–091939) and eyewalls after landfall (091940–100430). It is noted that the classification of these four segments is only based on the microphysical variations. The corresponding characteristic values for each segment are listed in Table 1.

Table 1. Microphysical characteristic values of raindrop size distributions for the entire period and four specific stages of Typhoon Morakot. The values are the mean for specific periods. The numbers in the parentheses show the coefficient of variation which is defined as 100% times the standard deviation divided by the mean value.

Drop spectra-based parameters	Entire	Stage-1 (072025-081035)	Stage-2 (081054-091619)	Stage-3 (091620-091939)	Stage-4 (091940-100430)
		outer rainbands, intermittent, stratiform	eyewall before landfall, continuous, convective	eye region, stratiform	eyewall after landfall, continuous, mixed convective-stratiform
Rain rate (mm h^{-1})	6.8 (154)	1.4 (186)	10.2 (125)	0.3 (105)	3.6 (79)
Liquid water content (g m^{-3})	0.34 (125)	0.09 (162)	0.48 (103)	0.03 (90)	0.23 (73)
Drop number concentration (m^{-3})	460 (86)	228 (116)	470 (74)	137 (76)	650 (68)
Radar reflectivity (dBZ)	27.7 (41)	16.9 (68)	33.0 (28)	12.5 (60)	26.4 (24)
Maximum diameter (mm)	2.21 (39)	1.51 (38)	2.67 (30)	1.22 (24)	1.81 (21)
Mass-weighted mean diameter (mm)	1.30 (35)	0.97 (28)	1.54 (28)	0.82 (21)	1.05 (19)

The first segment lasted about 14 h intermittently and was caused by outer rainbands. If not considering the eye region, the first segment exhibited the entire event's smallest drop sizes where the mean maximum diameter was only 1.51 mm, the lowest number concentration of 228 drops m^{-3}, the minimum rain

intensity of 1.4 mm h^{-1}, the lowest liquid water content of 0.09 g m^{-3} and the radar reflectivity of 16.9 dBZ. Significant features for the first segment were the relatively low concentration and high variability of raindrop size spectra. Compared with other segments, the first segment had the largest coefficients of variation for all characteristic parameters, herein defined as 100% times the standard deviation divided by the mean value to measure the fluctuating magnitude, indicating a strong intra-phase variation. The outer rainband generally takes on a more stratiform or a mixed convective-stratiform structure. As shown in Figure 4, the radar reflectivity from the National Aeronautic and Space Administration CloudSat satellite reveals that the outer rainband of Morakot had obvious stratiform structures (hint of brightband at the 4–5-km level). Figure 3e also confirms the stratiform characteristics since the sample's N_w is smaller than that of Bringi et al.[24]. The N_w and D_m derived from the composite size spectra for this segment (Figure 5) were 1786.7 m^{-3} mm^{-1} (3.25 in logarithmic scale) and 1.24 mm, respectively. This N_w–D_m pair was located in the stratiform rain region suggested by Bringi et al.[24]. So large N_w and small D_m suggest that the stratiform rain for this segment was formed by the melting of graupel or rimed ice particles. And these graupel and rimed ice particles in outer rainbands likely originated from the eyewall clouds[25].

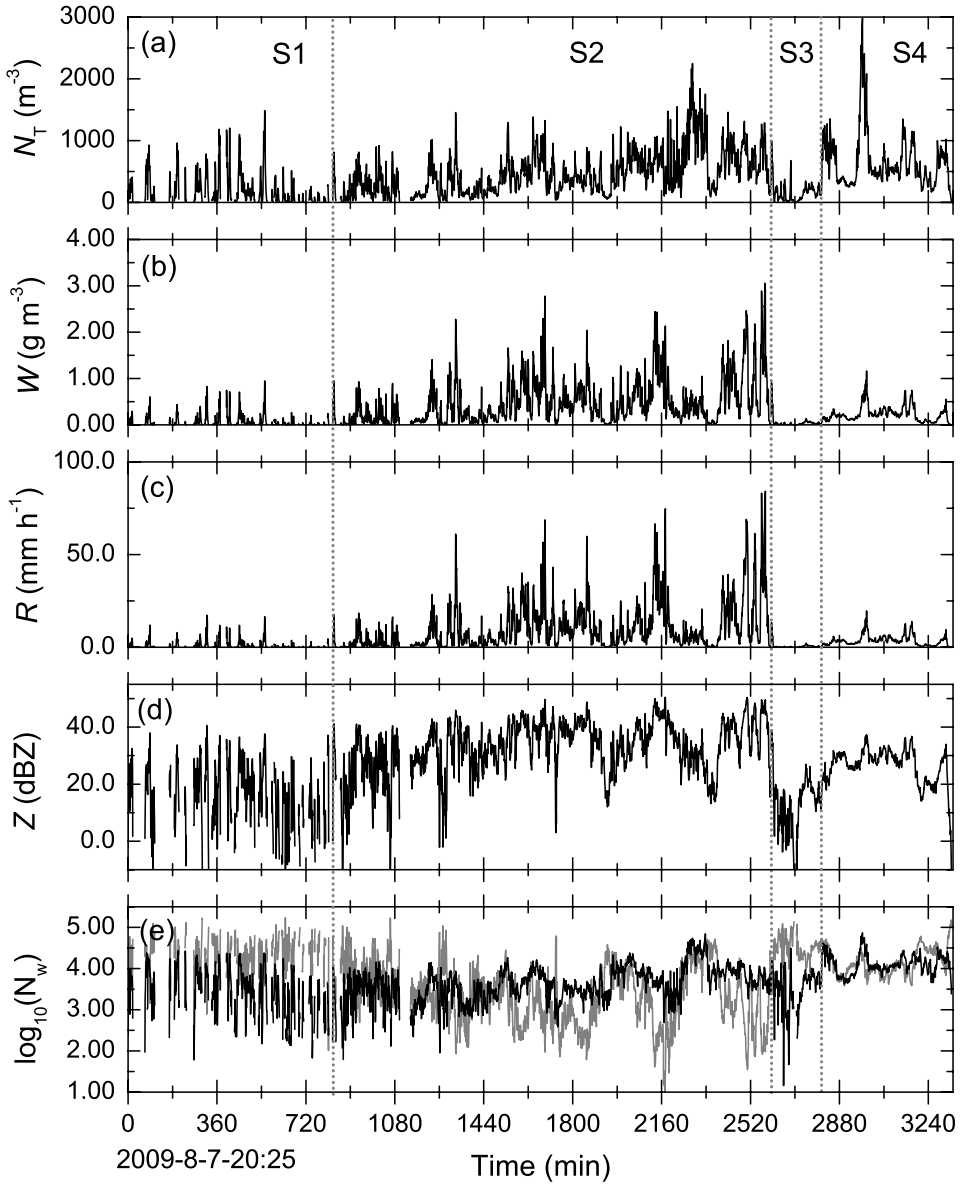

Figure 3. Temporal evolution of (a) total number concentration N (m^{-3}), (b) liquid water content W (g m^{-3}), (c) rain rate R (mm h^{-1}), (d) radar reflectivity factor Z (dBZ), and (e) normalized number concentration N_w (mm^{-1} m^{-3}, shown by the $\log_{10}N_w$), derived from 1–min disdrometer observations. The N_w corresponding to the regression N_w–D_m relation of Bringi et al.[24] for stratiform rain is given in gray line in panel (e). Symbols S1–4 represent four stages of the precipitation event.

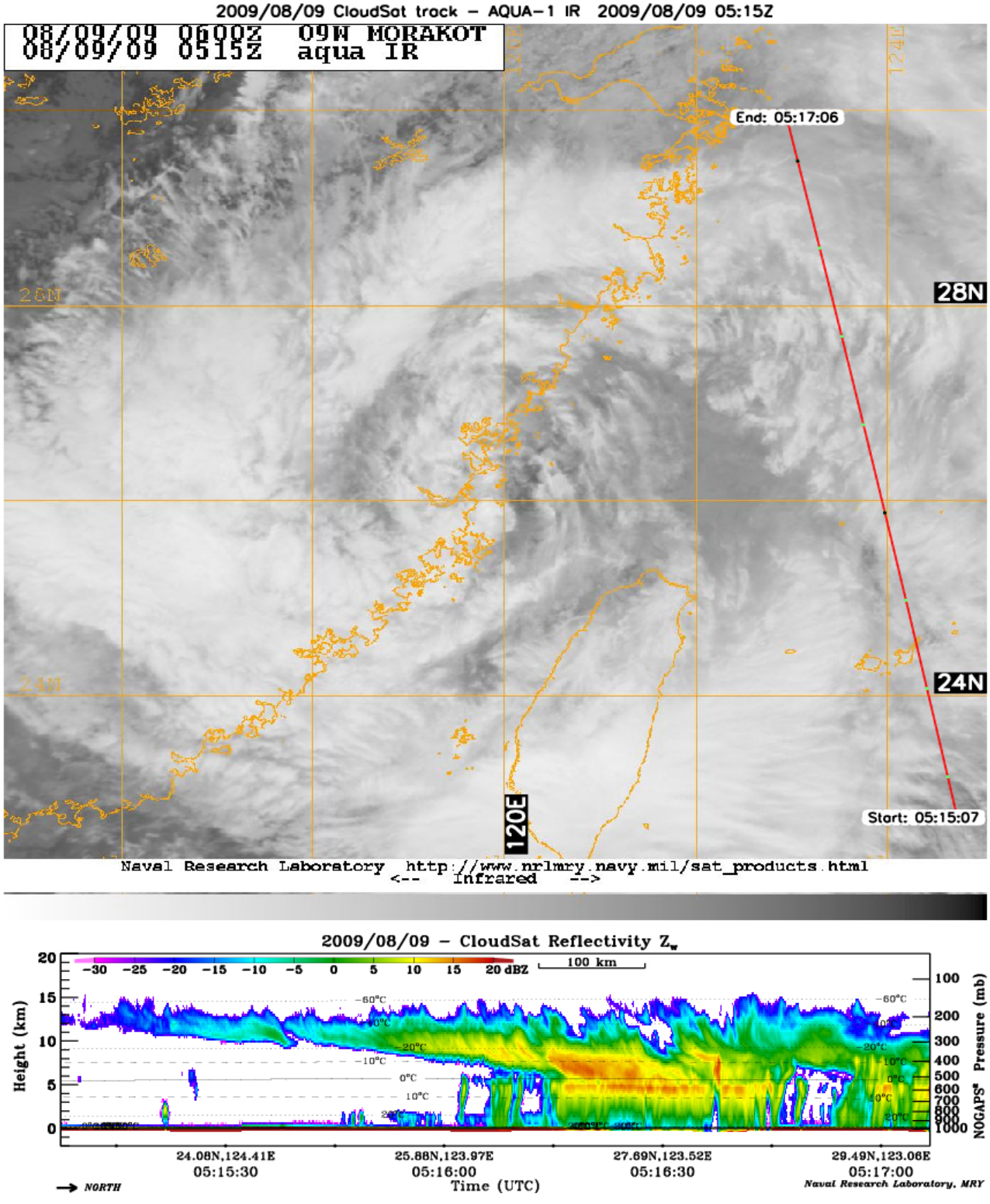

Figure 4. AQUA IR image at 0515 UTC 9 August 2009. CloudSat reflectivity from 0515 UTC to 0517 UTC is shown at bottom (courtesy of Naval Research Laboratory, Monterey, California), indicating the typical stratiform characteristics (hint of bright band at the 4–5-km level) for the outer rainbands.

The second segment lasted over 29 h continuously and was dominated by convective rains, showing relatively higher number concentrations, rain rates, liquid water contents, radar reflectivity and larger drop sizes. The number concentrations in this period were 470 m^{-3} in average and 2250 m^{-3} in maximum. This segment exhibited the event's broadest size spectra where the maximum drop diameter was 5.25 mm and the strongest rainfall with a maximum rain rate of about 84 mm h^{-1} and the

reflectivity of 50 dBZ. The relatively high concentrations of midsize drops (1~2 mm in diameter) with the presence of large drops were responsible for the heavy rain and high reflectivity (Figures 5 and 6). This is similar to those observed in Atlantic and the central tropical Pacific cyclones[14]. Precipitation for the second segment was caused by eyewall clouds through coalescence of drops. As shown in Figure 6, relatively small concentrations of raindrops with 1.2 mm in diameter were present in the broad raindrop spectra. This illustrates the presence of the coalescence of drops. The third segment lasted about 3.5 h and exhibited the event's smallest concentration with a mean value of 137 drops m^{-3}, the minimum rain intensity of ~0.3 mm h^{-1} and the lowest liquid water content of ~0.03 g m^{-3}. This segment had the storm's narrowest raindrop spectra with the maximum drop diameter not exceeding 2.4 mm (Figure 5). The clouds in the eye region of the tropical cyclones are mainly in the form of stratus and/or stratocumulus clouds[25], which is typically characterized by stratiform rains. Figure 3 illustrates this point further since the sample's N_w was significantly smaller than that of Bringi et al.[24]. The mean values were 3.5 (in logarithmic scale) for N_w and 0.82 mm for D_m, suggesting that the precipitation was formed by the melting of graupel or rimed ice particles. And these ice particles were likely produced in the eyewall clouds and hereafter advected inward into the eye region.

The last segment lasted about 9 h and exhibited weak convective rains, which are caused by stratiform clouds with embedded convection. The presence of high concentrations of small drops was observed in the narrow spectra where the maximum drop was less than 3 mm in diameter. However, compared with the second segment, the last segment had relatively weaker rainfall rates with a mean value of 3.6 mm h^{-1} and a lower liquid water content of 0.23 g m^{-3}. Although these two segments were caused by the eyewall clouds, the difference in rainfall features showed asymmetric structures of the storm.

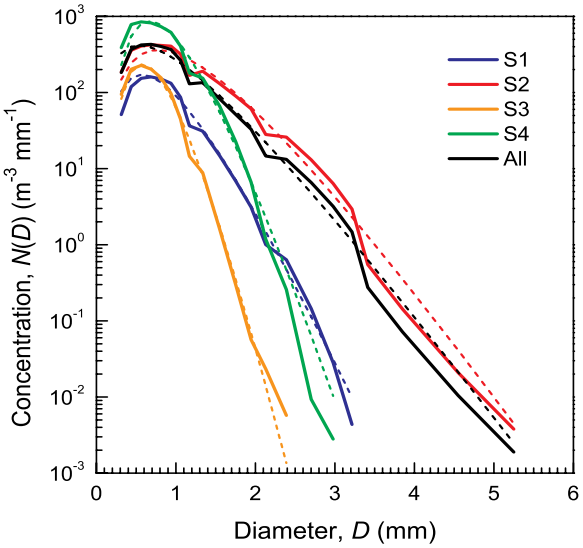

Figure 5. The composite raindrop size distributions (solid lines) for the whole dataset and four different segments. The dashed lines represent a gamma functional fit using the truncated moment method and the corresponding parameters are presented in Table 2.

Overall, during the passage of Morakot, the time series of the disdrometer data revealed four different segments associated with the evolution of the storm. Although all composite spectra were characterized by a single peak distribution in which the high concentration of drops occurred at 0.5–0.7 mm, the spectra width was significantly different from each other (Figure 5), resulting in different distribution parameters (Table 2).

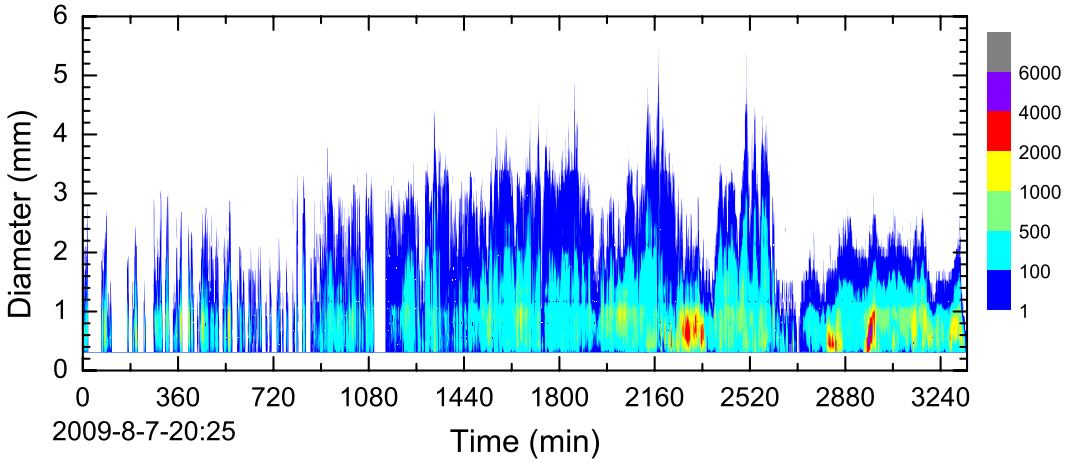

Figure 6. Time series (minutes from 2025 BST 7 August 2009) of raindrop size distribution (m^{-3} mm^{-1}) for Typhoon Morakot.

Table 2. The gamma distribution parameters based on the composite spectra in Figure 5.

	N_0 ($mm^{-1-\mu}$ m^{-3})	μ	Λ (mm^{-1})
Entire	8473.42	1.86	3.45
Stage-1	32542.94	3.36	5.88
Stage-2	14023.42	2.90	3.76
Stage-3	1.11×10^7	6.91	12.07
Stage-4	2.97×10^6	5.81	8.67

4 RAINDROP SIZE DISTRIBUTION PARAMETERIZATIONS

In this section, we would investigate the relationship of the gamma distribution parameters μ and Λ, and the radar reflectivity Z and rain rate R. Although the gamma distribution function has been widely used in the NWP models to describe a variety of drop size distributions, the shape parameter μ is often assumed to be a fixed constant. Based on the disdrometer and polarimetric radar data obtained from an intense convective rainfall with rain rate greater than 5 mm h^{-1}, Brandes et al.[26] and Zhang et al.[27] suggested an empirical relation between Λ and μ using a polynomial of second degree given by

$$\Lambda = 0.0365\mu^2 + 0.735\mu + 1.935 \quad (9)$$

For typhoon systems, Chang et al.[15] found that the μ–Λ relationship had a smaller slope under the same threshold of rain rate given by

$$\Lambda = 0.0136\mu^2 + 0.6984\mu + 1.5131 \quad (10)$$

Comparing Eq. (10) with Eq. (9), Chang et al.[15] suggested that the microphysical processes in typhoon systems under terrain influence was different than the system observed in east-central Florida.

In this research, after removing any raindrop size distributions in which the rain rate was less than 5 mm h^{-1}, the μ–Λ relationship for Typhoon Morakot was derived as

$$\Lambda = 0.0253\mu^2 + 0.633\mu + 1.524 \quad (11)$$

Comparisons of the fitting results (shown by solid curve) with Zhang et al.[27] (dashed–dotted curve) and Chang et al.[15] (dashed curve) are presented in Figure 7. As shown, the μ–Λ relationship for Morakot exhibits a significant difference with Zhang et al.[27], but is in excellent agreement with Chang et al.[15].

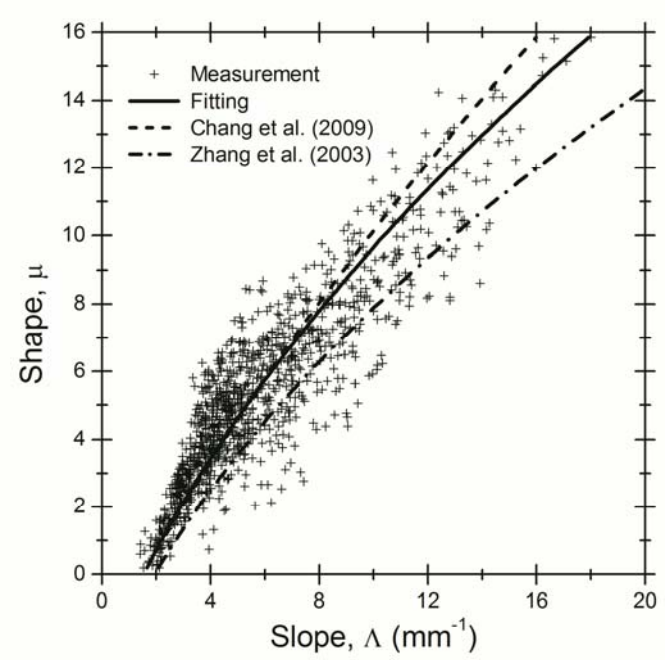

Figure 7. Scatterplot of the gamma parameters μ versus Λ for rainfall rates greater than 5 mm h^{-1}. Comparisons of the empirical μ and Λ relations obtained in this study (solid curve) and by Zhang et al. (2003) (dashed–dotted curve) and by Chang et al. (2009) (dashed curve).

Figure 8 shows a scatterplot of the values of the radar reflectivity factor Z and the rain rate R for the whole data set. We have also derived the empirical power-law Z–R relationships in the form $Z=AR^b$ using a least-square method. The coefficient of A and b was 235 and 1.3, respectively. For eyewall precipitation during the second segment, we obtained A=308 and b=1.32. Those values were consistent with those

reported in the literature for Atlantic hurricanes given by A=300 and b=1.35[28].

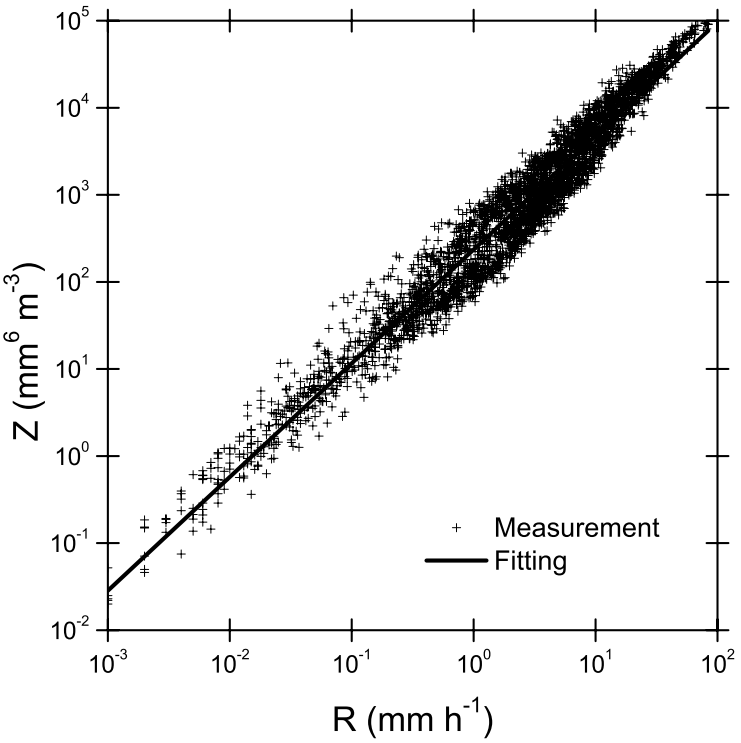

Figure 8. Scatterplot of radar reflectivity factor Z (mm^6 m^{-3}) versus rain rate R (mm h^{-1}) for the whole dataset. Straight line represents a least squares fit.

5 SUMMARY

In this study, the microphysical characteristics of drop size distributions during the passage of Typhoon Morakot were investigated using the PARSIVEL disdrometer data collected in Fujian province, China, from 7 to 10 August 2009. The time evolution of the raindrop size distribution revealed different segments of the observed storm. The outer rainbands and eye region produced stratiform rains while the eye walls produced convective rains. Overall, the Morakot precipitation exhibited a relatively high variability, especially before the landfall (Table 1).

All of the composite raindrop spectra for different segments and the entire period were characterized by a single peak distribution in which the high concentration of drops occurred at 0.5–0.7 mm, and well represented by the gamma distribution function. The eyewall precipitation had a broader size distribution than the outer rainband and eye region, resulting in a smaller slope.

The μ–Λ relation for Morakot derived here is in excellent agreement with the typhoon systems over Taiwan reported in Chang et al.[15]. The Z–R relation for Morakot during the eyewall stage is consistent with that of Atlantic hurricanes[28]. Specifically, the value is 308 for A and 1.32 for b.

Based on the N_W–D_m relationships, we suggest that the stratiform rain for the outer rainband and eye region was formed by the melting of graupel or rimed ice particles, which likely originated from the eyewall clouds.

It should be noted that the results presented in this study are based on one disdrometer measurement, which represents the time evolution of the raindrop size distribution over a single site. More observation sites are needed to measure the spatial variability of microphysical characteristics of tropical cyclone precipitation.

Acknowledgement: The first author would like to thank Dr. Guifu Zhang at University of Oklahoma for providing the source code of the truncated moment method.

REFERENCES:

[1] HONG C C, LEE M Y, HSU H H, et al. Role of submonthly disturbance and 40-50 day ISO on the extreme rainfall event associated with Typhoon Morakot (2009) in Southern Taiwan [J]. Geophys. Res. Lett., 2010, 37, L08805, doi:10.1029/2010GL042761.

[2] ZHANG F, WENG Y, KUO Y-H, et al. Predicting typhoon Morakot's catastrophic rainfall with a convection-permitting mesoscale ensemble system [J]. Wea. Forecasting, 2010, 25(6): 1816-1825.

[3] CHIEN F C, KUO H C. On the extreme rainfall of Typhoon Morakot (2009) [J]. J. Geophys. Res., 2011, 116, D05104, doi:10.1029/2010JD015092.

[4] LIU C C, LIU G R, LIN T H, et al. Accumulated rainfall forecast of Typhoon Morakot (2009) in Taiwan using satellite

data [J]. J. Meteor. Soc. Japan, 2010, 88(5): 785-798.
[5] EBERT E E, TURK M, KUSSELSON S J, et al. Ensemble tropical rainfall potential (eTRaP) forecasts [J]. Wea. Forecasting, 2011, 26(2): 213-224.
[6] NGUYEN H V, CHEN Y L. High-resolution initialization and simulations of Typhoon Morakot (2009) [J]. Mon. Wea. Rev., 2011, 139(5): 1463-1691.
[7] ATLAS D, ULBRICH C W. Drop size spectra and integral remote sensing parameters in the transition from convective to stratiform rain [J]. Geophys. Res. Lett., 2006, 33, L16803, doi:10.1029/2006GL026824.
[8] CHAPON B, DELRIEU G, GOSSET M, et al. Variability of rain drop size distribution and its effect on the Z–R relationship: A case study for intense Mediterranean rainfall [J]. Atmos. Res., 2008, 87(1): 52-65.
[9] MARTNER B E, YUTER S E, WHITE A B, et al. Raindrop size distributions and rain characteristics in California coastal rainfall for periods with and without a radar bright band [J]. J. Hydrometeor., 2008, 9(3): 408-425.
[10] MOUMOUNI S, GOSSET M, HOUNGNINOU E. Main features of rain drop size distributions observed in Benin, West Africa, with optical disdrometers [J]. Geophys. Res. Lett., 2008, 35, L23807, doi:10.1029/2008GL035755.
[11] LEE C K, LEE G W, ZAWADZKI I, et al. A preliminary analysis of spatial variability of raindrop size distributions during stratiform rain events [J]. J. Appl. Meteor. Climatol., 2009, 48(2): 270-283.
[12] NIU Sheng-jie, JIA Xing-can, SANG Jian-ren, et al. Distributions of raindrop sizes and fall velocities in a semiarid plateau climate: Convective versus stratiform rains [J]. J. Appl. Meteor. Climatol., 2010, 49(4): 632-645.
[13] TAPIADOR F J, CHECA R, DE CASTRO M. An experiment to measure the spatial variability of rain drop size distribution using sixteen laser disdrometers [J]. Geophys. Res. Lett., 2010, 37, L16803, doi:10.1029/2010GL044120.
[14] TOKAY A, BASHOR P G, HABIB E, et al. Raindrop size distribution measurements in Tropical Cyclones [J]. Mon. Wea. Rev., 2008, 136(5): 1669-1685.
[15] CHANG W Y, WANG T C C, LIN P L. Characteristics of the raindrop size distribution and drop shape relation in typhoon systems in the western Pacific from the 2D video disdrometer and NCU C-band polarimetric radar [J]. J. Atmos. Ocean Technol., 2009, 26(10): 1973-1993.
[16] BATTAGLIA A, RUSTEMEIER E, TOKAY A, et al. PARSIVEL snow observations: A critical assessment [J]. J. Atmos. Ocean Technol., 2010, 27(2): 333-344.
[17] YUTER S E, KINGSMILL D E, NANCE L B, et al. Observations of precipitation size and fall speed characteristics within coexisting rain and wet snow [J]. J. Appl. Meteor., 2006, 45(10): 1450-1464.
[18] CHEN Bao-jun, HU Wen, PU Jiang-ping. Characteristics of the raindrop size distribution for freezing precipitation observed in southern China [J]. J. Geophys. Res., 2011, 116, D06201, doi:10.1029/2010JD015305.
[19] LÖFFLER-MANG M, BLAHAK U. Estimation of the equivalent radar reflectivity factor from measured snow size spectra [J]. J. Appl. Meteor., 2001, 40(4): 843-849.
[20] LÖFFLER-MANG M, JOSS J. An optical disdrometer for measuring size and velocity of hydrometeors [J]. J. Atmos. Oceanic Technol., 2000, 17(2): 130-139.
[21] GUNN R, KINZER G D. The terminal velocity of fall for water droplets in stagnant air [J]. J. Meteor., 1949, 6(4): 243-248.
[22] ULBRICH C W. Natural variations in the analytical form of the raindrop size distribution [J]. J. Clim. Appl. Meteor., 1983, 22(10): 1764-1775.
[23] VIVEKANANDAN J, ZHANG G, BRANDES E. Polarimetric radar estimators based on a constrained gamma drop size distribution model [J]. J. Appl. Meteor., 2004, 43(2): 217-230.
[24] BRINGI V N, CHANDRASEKAR V, HUBBERT J, et al. Raindrop size distribution in different climatic regimes from disdrometer and dual-polarized radar analysis [J]. J. Atmos. Sci., 2003, 60(2): 354-365.
[25] HOUZE R A Jr. Clouds in tropical cyclones [J]. Mon. Wea. Rev., 2010, 138(2): 293-344.
[26] BRANDES E A, ZHANG G, VIVEKANANDAN J. An evaluation of a drop distribution–based rainfall estimator [J]. J. Appl. Meteor., 2003, 42(5): 652-660.
[27] ZHANG G, VIVEKANANDAN J, BRANDES E A, et al. The shape–slope relation in observed gamma raindrop size distributions: Statistical error or useful information? [J]. J. Atmos. Oceanic Technol., 2003, 20(8): 1106-1119.
[28] JORGENSEN D P, WILLIS P T. A Z-R relationship for hurricanes [J]. J. Appl. Meteor., 1982, 21(3): 356-366.

Citation: CHEN Bao-jun, WANG Yuan and MING Jie. Microphysical characteristics of the raindrop size distribution in typhoon Morakot (2009). *J. Trop. Meteor.*, 2012, 18(2): 162-171.